A Modern Look at Conformal Mapping Including Multiply Connected Regions

David C. Ives*
Grumman Aerospace Corporation, Bethpage, N.Y.

With the advent of large-scale digital computers, numerical solution of the transonic flow equations in two dimensions has proven feasible. In such calculations it is convenient, and often crucial, to map the region of interest conformally onto a simple domain so that a simple finite difference system can be employed. This paper updates a well-known airfoil conformal mapping method (Theodorsen and Garrick) with modern techniques, greatly enhancing the mapping speed and accuracy while simplifying the analysis. Also, a powerful new class of conformal transformations is introduced, and applied to a two-element airfoil.

Introduction

IN the calculation of transonic flow over airfoils it has proven convenient to map the infinite region of the flow exterior to an airfoil conformally onto a finite region, such as the interior of a circle, as in Sells,[1] Melnik and Ives,[2] Jameson,[3] and Bauer, Garabedian, and Korn.[4]

Such a mapping places a fine grid in the physical plane where needed, while retaining a uniform grid in the (conformally mapped) computational plane. The gradients of flow properties in the computational plane are smaller than in the physical plane, so that finite difference approximations in the computational plane are more accurate than in the physical plane. This allows the use of a rather coarse grid. It is easier to apply boundary conditions in the mapped plane than it is in the physical plane, as the boundaries are coordinate lines in the mapped plane. The conformal mapping ensures that the nonlinear partial differential equations in the computational plane are only slightly more complicated than those in the physical plane.[1-5] To take advantage of the above considerations, there is a need for conformal mapping techniques that are simple and rapid.

This paper presents a conformal mapping technique which is at least an order of magnitude faster than conventional mapping techniques. In analogy to the fast Fourier transform techniques utilized here, the present work can be considered a "fast conformal mapping."

This paper also introduces a powerful new class of conformal transformations. These new transformations are an extension of the well-known von Karman-Trefftz transformation to multiply-connected regions, and can be used in the analysis of flow over multielement airfoils. They have the property that any number N of airfoil elements are simultaneously (with one application of the transformation) mapped to N near circles.

One member of this new class of transformations is used in mapping the region exterior to a two-element airfoil onto the region between two concentric circles. By combining the known solution for incompressible flow between two concentric circles[6] with this two-element mapping, we can very simply solve for the inviscid incompressible flow over a two-element airfoil.

Single-Element Airfoil Mapping—A Modern View

We present here a modern look at the mapping of a single-element airfoil, proceeding along the lines of Theodorsen and Garrick.[7] In some of the figures, a secondary airfoil is carried through the transformations for later reference in the section on the two-element airfoil mapping technique.

The problem of conformally mapping, with high accuracy, a point-by-point representation of an airfoil onto a circle can be broken down into at least four distinct steps. The first of these steps is to remove effects of slope discontinuties in the airfoil contour and expand regions of rapid flow change (such as the nose region) by analytically mapping the airfoil, point by point, onto a nearly circular, smooth contour. The second step is a coordinate system translation to place the centroid of the near circle on (or near) the origin. The third step is to obtain a continuous representation of the near-circle contour, and thus of the airfoil, by interpolation. The fourth step is to map this nearly circular contour onto a circle.

For the first of these steps, we employ a von Karman-Trefftz transformation,[8] which may be written as

$$\frac{Z_2 - S_1}{Z_2 + S_1} = \left(\frac{Z_1 - Z_{S1} - \kappa_1 \cdot S_1}{Z_1 - Z_{S1} + \kappa_1 \cdot S_1} \right) \frac{1}{\kappa_1} \tag{1}$$

where Z_1 = airfoil plane complex coordinate; Z_2 = near-circle plane complex coordinate; $\kappa_1 = 2 - \tau_1/\pi$; τ_1 = trailing edge included angle; Z_{S1} = complex constant; and S_1 = complex constant.

This transformation is singular at

$$Z_1 = Z_{S1} + \kappa_1 \cdot S_1 \equiv Z_{1T}$$

and

$$Z_1 = Z_{S1} - \kappa_1 \cdot S_1 \equiv Z_{1N}$$

The two singular points, Z_{1T} and Z_{1N}, are placed in the Z_1 plane at the trailing edge and at a point midway between the nose of the airfoil and its center of curvature, as illustrated in Fig. 1. This determines the parameters S_1 and Z_{S1} so that the trailing edge included angle is opened up to 180° and the airfoil is transformed into a nearly circular contour.

The von Karman-Trefftz transformation contains a fractional power, so care must be exercised in choosing the correct branch. This is accomplished by "tracking" the transformation from a point where it is known to the point of interest. This involves enforcing the continuity of the argument of the base in Eq. (1) along a path not crossing the boundary of the airfoil. This process may be initialized by noting that, as Z_1 approaches infinity, the argument of the base approaches zero. A simple and efficient implementation of tracking along the airfoil due to Korn is presented in the program listing of Ref. 9.

The second step shifts and coordinate system origin to the centroid of the near circle. This shift is accomplished using

Presented as Paper 75-842 at the AIAA 8th Fluid and Plasmadynamics Conference, Hartford, Conn., June 16-18, 1975; submitted June 27, 1975; revision received December 1, 1975.

Index categories: Aircraft Aerodynamics (including Component Aerodynamics); Hydrodynamics; Subsonic and Transonic Flow.

*Associate Research Scientist, Scientific Analysis Group, Pratt and Whitney Aircraft, East Hartford, Conn. Member AIAA.

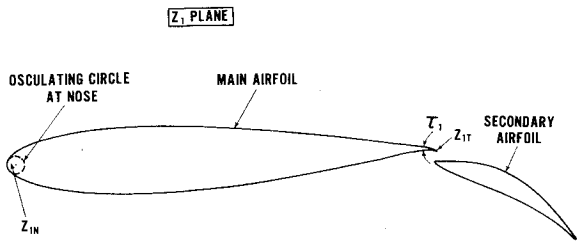

Fig. 1 Airfoil geometry.

an approximate centroid obtained by connecting adjacent points with straight lines and calculating the centroid of the resulting figure. This transformation is written as

$$Z_2' = Z_2 - C_2 \tag{2}$$

where C_2 is the centroid location in the Z_2 plane. This improves the convergence of a series expansion to be used in the fourth step.

The third step is to obtain a continuous representation of the airfoil image which has been defined pointwise by the previous transformations. This is done by adopting a polar coordinate system as defined in Fig. 2, and fitting ln r as a function of θ with a periodic cubic spline. This curve fitting technique has properties that result in a smooth definition of the airfoil image with a high interpolation accuracy. The algorithm used is a direct adaptation of the equations presented in Ahlberg, Nilson, and Walsh.[10]

The fourth step is the transformation of the near circle to a circle with the Theodorsen-Garrick transformation. Typical results are illustrated in Figs. 2 and 3. The approach used here follows the Theodorsen-Garrick approach,† except that the Fourier analysis and synthesis required are performed as described in Cooley, Lewis, and Welch[11] utilizing fast Fourier techniques first introduced by Cooley and Tukey[12] in 1965. It is interesting to note that Eq. (14.9) of Garrick[13] could have directly used fast Fourier techniques, had they been available in 1949.

The Theodorsen-Garrick transformation may be written, for N a finite number, as

$$Z_2' = Z \exp\left[\sum_{j=0}^{N} (A_j + iB_j)(Z)^{-j} \right] \tag{3}$$

The near circle, represented in polar coordinates, is

$$Z_2' = r(\theta) e^{i\theta} \tag{4}$$

The desired image of the airfoil in the circle plane, which we denote as the Z plane, is the unit circle‡

$$Z = e^{i\phi} \tag{5}$$

By substituting these polar representations into Eq (3), taking the logarithm of both sides, and separating into real and imaginary parts, the following equations are obtained:

$$\ln r = A_0 + \sum_{j=1}^{N} [A_j \cos(j\phi) + B_j \sin(j\phi)] \tag{6}$$

†While Theodorsen and Garrick found it expedient to work with an integral equation with a contangent kernel, the approach here is to work directly with the Fourier series to take advantage of fast Fourier techniques.

‡For matters of convenience in the next section the present approach produces a unit circle in the Z plane with the mapping modulus not unity at infinity, while the Theodorsen-Garrick approach produces a non-unit circle with the mapping modulus unity at infinity. Of course, the two approaches are equivalent, being related by a simple magnification.

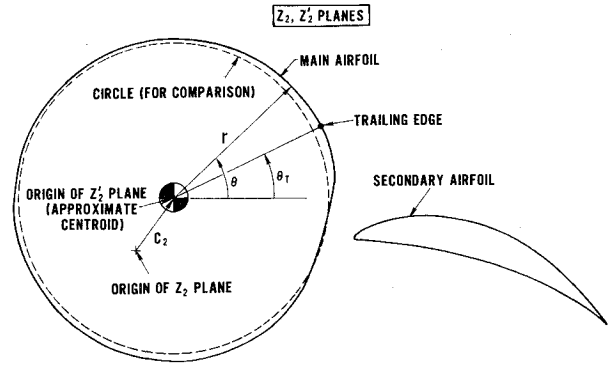

Fig. 2 Main airfoil mapped to a near circle.

$$\theta = \phi + B_0 + \sum_{j=1}^{N} [B_j \cos(j\phi) - A_j \sin(j\phi)] \tag{7}$$

On the near circle, ln r is known as a function of θ from the periodic cubic spline fit. The problem is to determine the coefficients A_j and B_j, which is accomplished using fast Fourier techniques and an iteration process.

Consider $2N$ points on the circle in the Z plane starting at the trailing edge and equally spaced around the circle, so that

$$\phi_k = 2\pi(k-1)/2N \quad k = 1,\ldots,2N \tag{8}$$

To place the trailing edge in the Z plane at $\phi = 0$, set

$$B_0 + \sum_{j=1}^{N} B_j = \theta_T \tag{9}$$

where θ_T is the value of θ at the trailing edge in the Z_2' plane. To close the system we are free to set

$$B_N = 0 \tag{10}$$

Then, θ_k is given by

$$\theta_k - \phi_k = \theta_T - \sum_{j=1}^{N-1} B_j + \sum_{j=1}^{N-1} [B_j \cos(j\phi_k) - A_j \sin(j\phi_k)] \tag{11}$$

Equation (11) may be evaluated (given A_j, B_j, for $j = 1,\ldots,N-1$) by Fourier techniques as follows:

$$y_1 = \tfrac{1}{2}(\theta_T - \sum_{j=1}^{N-1} B_j) \tag{12a}$$

$$y_{j+1} = \tfrac{1}{2}(B_j + iA_j) \quad j = 1,\ldots,N-1 \tag{12b}$$

$$y_{2N-j+1} = \bar{y}_j \quad j = 1,\ldots,N \tag{12c}$$

where the bar "—" denotes a complex conjugate. It may be shown[11] that

$$\theta_k - \phi_k = \sum_{j=1}^{2N} y_j \exp\left[2\pi i \frac{(j-1)(k-1)}{2N} \right] \tag{12d}$$

Equation (12d) is known as a "discrete Fourier transform" in the literature.[11,12] It may be evaluated using fast Fourier techniques in 0 ($N \ln_2 N$) operations for $k = 1,\ldots,N$ as compared with 0 (N^2) operations required for a straightforward evaluation of Eq. (11).

A similar technique can be applied to Eq. (6) to obtain the A_j and B_j corresponding to a trigonometric series fit through the points $(\ln r)_k$ for $k = 1,\ldots,2N$ as follows: define

$$y_j = \frac{1}{2N} \sum_{k=1}^{2N} (\ln r)_k \exp\left[-2\pi i \frac{(j-1)(k-1)}{2N} \right] \tag{13a}$$

then we have[11]

$$A_j = 2\ Re\ (y_{j+1}) \quad j=0,\ldots,N \tag{13b}$$

$$B_j = -2Im(y_{j+1}) \quad j=1,\ldots,N-1 \tag{13c}$$

where $(\ln r)_k$ is the value of $\ln r$ at the kth point given by Eq. (8). Equation (13a) is easily evaluated in $0(N \ln_2 N)$ operations using fast Fourier techniques.

An iteration then may be summarized as follows: 1) set $A_j = B_j = 0$ for $j=1,\ldots,N-1$; 2) evaluate θ_k using Eqs. (12a-12d); 3) evaluate $(\ln r)_k$ for $k=1,\ldots,2N$ using θ_k and the spline fit coefficients; 4) solve for A_0, A_N, and A_j, B_j for $j=1,\ldots,N-1$ using Eqs. (13a-13c); 5) using the latest values for the A_j, B_j, repeat steps 2-4 until convergence is achieved. The resulting image in the Z plane, along with the secondary foil, is illustrated in Fig. 3.

It has been shown by Warschawski[14] that sufficient conditions for convergence of the above iteration are

$$(r_{max}/r_{min})^{1/2} - 1 < \epsilon$$

$$\left| \left(\frac{\partial \ln r}{\partial \theta} \right)_{max} \right| < \epsilon$$

where $\epsilon = 0.2954976$. The subscripts refer to maximum and minimum values on the near circle in the Z_T' plane.

The overall accuracy of this mapping is limited by the accuracy obtainable in each separate step. The first two steps involve no approximations, and are exact to the accuracy of the computer. The fourth step is limited in accuracy by the ability of a trigonometric series with a finite number of terms to represent a given continuous periodic function. An error analysis by Abramovici[15] indicates that with about 100 terms, we should be able to represent $\ln r$ as a trigonometric series in θ with an accuracy equal to the roundoff error of an IBM 370 in single precision. Because of the shift in the coordinate system in step 2, the terms in the Theodorsen-Garrick series decrease very rapidly. With 100 terms, the last few are typically of the same order as the computer roundoff. Thus, the fourth step can be carried out with an accuracy essentially to that of the computer roundoff error.

The third step, where a periodic cubic spline is used to interpolate ln r as a function of θ, is thus seen to contribute the dominant "errors," if they may be called errors. These interpolation "errors" are small, as the interpolation is of high order and is performed on a slowly varying smooth function. Actually these "errors" stem from the airfoil being specified only at a finite number of points. In any case, the transformations map these given airfoil points onto a circle with an accuracy limited only by computer roundoff. In summary, the method presented here is essentially exact, being limited only by the method in which the airfoil is defined between the specified coordinates.

An IBM 370/165 computer will typically require 3 sec of central processor time to map a single element airfoil conformally to a circle using 100 terms in the Theodorsen-Garrick series. With this number of terms, the specified input coordinates are mapped to a circle with 5-digit accuracy.

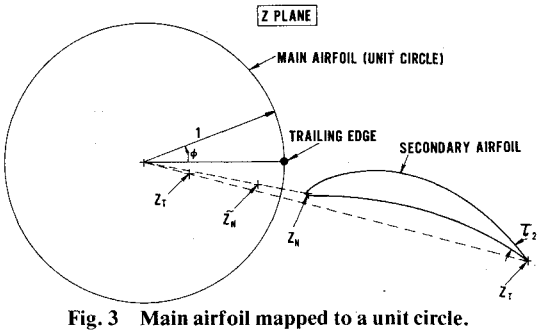

Fig. 3 Main airfoil mapped to a unit circle.

Two-Element Airfoil Mapping

The basic work on the mapping of two-element airfoils is that of Garrick.[16] The approach followed here retains some features of his work, while taking a novel approach to the problem based on a new transformation.

The two-element mapping is initially identical to the single-element airfoil mapping, except that we "carry along" the secondary foil through the first four steps (as illustrated in Figs. 1-3). We then transform the resulting airfoil-like shape representing the secondary foil to a near circle, *while keeping the image of the main foil a circle,* with the new transformation

$$\frac{\zeta-\zeta_T}{\zeta-\zeta_N} \cdot \frac{\zeta-\tilde{\zeta}_T}{\zeta-\tilde{\zeta}_N} = \left(\frac{Z-Z_T}{Z-Z_N} \cdot \frac{Z-\tilde{Z}_T}{Z-\tilde{Z}_N} \right)^{1/\kappa_2} \tag{14}$$

where

$$\kappa_2 = 2 - \tau_2/\pi \tag{15a}$$

$$\tilde{Z}_T = 1/\bar{Z}_T \tag{15b}$$

$$\tilde{Z}_N = 1/\bar{Z}_N \tag{15c}$$

$$\tilde{\zeta}_T = R^2/\bar{\zeta}_T \tag{15d}$$

$$\tilde{\zeta}_N = R^2/\bar{\zeta}_N \tag{15e}$$

$$\frac{\zeta_T}{\zeta_N} \left(\frac{\bar{\zeta}_N}{\bar{\zeta}_T} \right) = \left[\frac{Z_T}{Z_N} \left(\frac{\bar{Z}_N}{\bar{Z}_T} \right) \right]^{1/\kappa_2} \tag{15f}$$

The scalar R is the circle radius in the ζ plane, τ_2 is the secondary foil trailing edge included angle, and Z_N, Z_T, ζ_N, and ζ_T are complex constants. Note that the points $\tilde{Z}_T$, $\tilde{Z}_N$, $\tilde{\zeta}_T$, and $\tilde{\zeta}_N$ are reflections of the points Z_T, Z_N, ζ_T, and ζ_N with respect to the circles of radius unity and R as illustrated in Figs. 3 and 4. In essence, we are using the method of images.

In a manner similar to the single-foil case, the singular points Z_T and Z_N are placed in the Z plane at the trailing edge and at a point midway between the nose of the secondary airfoil and its center of curvature, as illustrated in Fig. 3. This determines Z_T and Z_N (and thus $\tilde{Z}_T$ and $\tilde{Z}_N$) such that the secondary foil is mapped into a near circle.

A far-field analysis shows that $dZ/d\zeta \to 1$ as $\zeta \to \infty$ only if

$$\zeta_T - \zeta_N + \tilde{\zeta}_T - \tilde{\zeta}_N = (1/\kappa_2)\,(Z_T - Z_N + \tilde{Z}_T - \tilde{Z}_N) \tag{16}$$

Now consider the two transformations

$$f(Z) = \left(\frac{Z-Z_T}{Z-Z_N} \cdot \frac{Z-\tilde{Z}_T}{Z-Z_N} \right)^{1/\kappa_2} \tag{17a}$$

$$g(\zeta) = \frac{\zeta-\zeta_T}{\zeta-\zeta_N} \cdot \frac{\zeta-\tilde{\zeta}_T}{\zeta-\tilde{\zeta}_N} \tag{17b}$$

Examination of Eqs. (17a) and (17b) reveals $dZ/df \to \infty$ when

$$\frac{1}{Z-Z_N} - \frac{1}{Z-Z_T} + \frac{1}{Z-\tilde{Z}_N} - \frac{1}{Z-\tilde{Z}_T} = 0 \tag{18a}$$

and $d\zeta/dg \to \infty$ when

$$\frac{1}{\zeta-\zeta_N} - \frac{1}{\zeta-\zeta_T} + \frac{1}{\zeta-\tilde{\zeta}_N} - \frac{1}{\zeta-\tilde{\zeta}_T} = 0 \tag{18b}$$

We denote the roots of Eqs. (18a) and (18b) as the singular points Z_{01}, Z_{02}, ζ_{01}, and ζ_{02}. A more detailed analysis reveals that at these singular points the arguments of f and g are identical but in general the magnitudes of f and g are different. Thus we must have

$$\left| \left(\frac{Z_{01}-Z_T}{Z_{01}-Z_N} \cdot \frac{Z_{01}-\tilde{Z}_T}{Z_{01}-\tilde{Z}_N} \right)^{1/\kappa_2} \right| = \left| \frac{\zeta_{01}-\zeta_T}{\zeta_{01}-\zeta_N} \cdot \frac{\zeta_{01}-\tilde{\zeta}_T}{\zeta_{01}-\tilde{\zeta}_N} \right| \tag{19a}$$

$$\left|\left(\frac{Z_{02}-Z_T}{Z_{02}-Z_N}\cdot\frac{Z_{02}-\tilde{Z}_T}{Z_{02}-\tilde{Z}_N}\right)^{1/\kappa_2}\right|=\left|\frac{\zeta_{02}-\zeta_T}{\zeta_{02}-\zeta_N}\cdot\frac{\zeta_{02}-\tilde{\zeta}_T}{\zeta_{02}-\tilde{\zeta}_N}\right| \quad (19b)$$

otherwise $dZ/d\zeta$ or its inverse will be singular at these points.

Examination of the previous equations reveals that we have as unknowns the real variable R and complex variable ζ_N; the remaining quantities may be obtained from Eqs. (15a-15e) and (16). There are three real equations [(15f), (19a), and (19b)] that must be satisfied by the choice of R and ζ_N. This is easily implemented as a rapidly convergent Newton-Raphson iteration process.

It can be analytically demonstrated that the mapping as specified here transforms the secondary airfoil into a near circle, and transforms the image of the main airfoil (a unit circle) into a circle of radius R. This mapping is nonsingular at all points distinct from $Z_N, Z_T, \tilde{Z}_N, \tilde{Z}_T, \zeta_N, \zeta_T, \tilde{\zeta}_N$, and $\tilde{\zeta}_T$.

The near circle is subsequently mapped to a near circle interior to the unit circle with the bilinear transformation

$$Z_5 = a\cdot\frac{\zeta+b}{\zeta+c} \quad (20)$$

The trailing edge image of the main foil, denoted as ζ_{TE}, will transform to the point $Z_5 = 1$ if

$$a\cdot\frac{\zeta_{TE}+b}{\zeta_{TE}+c}=1 \quad (21)$$

The near circle image in the $Z5$ plane should be centered on the origin, so that a Fourier series, to be utilized later, will display rapid convergence. We thus require that ζ_C, which is the image in the ζ plane of the centroid of the near circle in the $Z5$ plane, transform into $Z_5 = 0$, so that

$$\zeta_c + b = 0 \quad (22)$$

The bilinear transform will map the circle of radius R centered on the origin in the ζ plane into a unit circle centered on the origin in the Z_5 plane if

$$1/\zeta_c + c = 0 \quad (23)$$

The complex constants a, b, and c are then determined as follows: 1) set ζ_C = centroid of near circle in ζ plane; 2) solve Eqs. (21-23) for a, b, and c; 3) using Eq. (20), transform the near circle from the ζ plane to the Z_5 plane; 4) calculate the approximate centroid of near circle in the Z_5 plane, denoted as Z_{5C}, by connecting adjacent points with straight lines and calculating the centroid of the resulting figure; 5) calculate a new value for ζ_C from Eq. (20), using Z_{5C}, a, b, and c; 6) using the latest value of ζ_C repeat steps 2-5 until convergence is achieved.

This process converges rapidly to the solution, at which Z_{5C} is zero. The region exterior to the two airfoils is mapped onto the region between the near circle and the circle. The region infinitely far from the airfoils in the ζ plane is mapped into the point denoted as "infinity" in Fig. 5.

The near circle at this stage is determined only point by point, so a periodic cubic spline is used to interpolate ln r on the near circle as a function of θ, as in the single-foil case. The transformation of the near circle to a circle, while keeping the image of the main foil a unit circle,§ is then accomplished with the transformation

$$\text{SUM}=\sum_{j=1}^{N}\left[(-A_{2j}+iB_{2j})(\hat{R}\cdot Z_6)^j+(A_{2j}+iB_{2j})(\hat{R}/Z_6)^j\right] \quad (24a)$$

§It is easily verified that "SUM" is purely imaginagy when $Z_6 = e^{i\beta}$ for any real value of β, thus Eq. (24) transforms a unit circle in the Z_6 plane to a unit circle in the Z_5 plane.

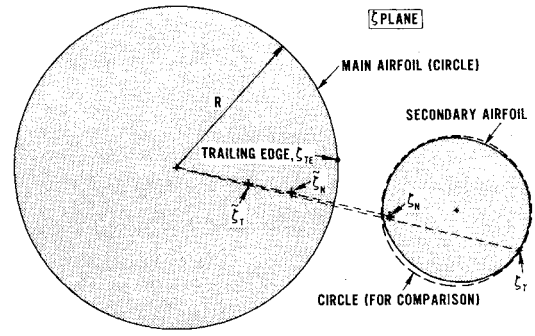

Fig. 4 Main airfoil remains a circle while secondary airfoil is mapped to near circle.

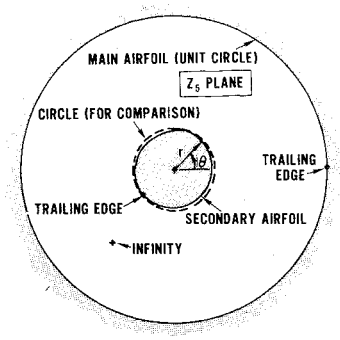

Fig. 5 Main airfoil remains a circle while near circle is moved to center.

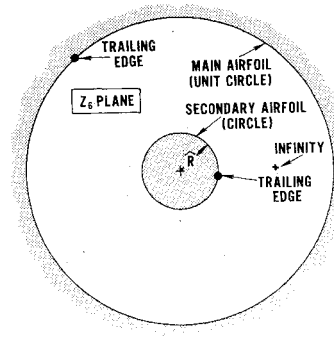

Fig. 6 Circle remains a circle while near circle is mapped to circle.

$$Z_5 = Z_6\exp(iB_{Z2}+\text{SUM}) \quad (24b)$$

where $\hat{R}$ is the radius of the image of the near circle in the Z_6 plane. This transformation is a special case of the Garrick[16] transformation. The grouping of the terms $(\hat{R}\cdot Z_6)$ and $(\hat{R}/Z_6)$ prevents roundoff error from destroying numerical significance. A method analogous to that of Garrick,[16] but using fast Fourier techniques as in the earlier part of this paper, can be employed to solve for the A_{2j} and B_{2j} in Eq. (24a). For convenience, the constant B_{Z2} in Eq. (24b) is chosen such that the point labeled "infinity" in Fig. 5 is mapped into a point on the positive real axis, as illustrated in Fig. 6. This completes the mapping.

This mapping has been performed on the coordinates given by Williams,[17] who provided an exact test case for flow over a two-element airfoil. This exact test case is, in fact, the case illustrated in this paper.

The Lagally solution[6] for incompressible flow between two concentric circles may be used to calculate the incompressible streamlines in the Z_6 plane. A plot of some of these streamlines is given in Fig. 7. By tracing the coordinates of these streamlines back through the transformations to the Z_1 plane, we obtain streamlines of flow over a two-element airfoil, as illustrated in Fig. 8. The Lagally solution, combined with the mapping developed here, made possible the rapid and accurate calculation of incompressible flow over a two-element airfoil. For the test case of Williams, 6 sec of IBM

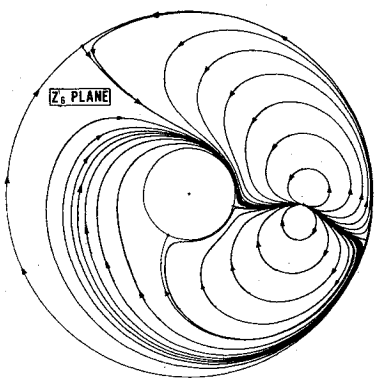

Fig. 7 Incompressible streamlines in Z_6 plane.

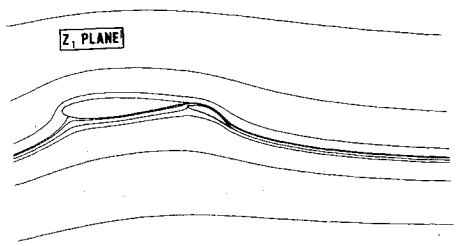

Fig. 8 Incompressible streamlines in Z_1 plane.

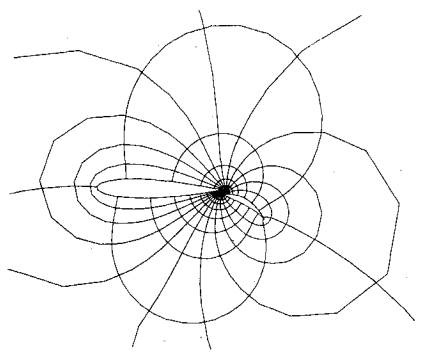

Fig. 9 Uniform polar coordinate grid in transformed plane transferred back to airfoil plane.

370/165 computer time were required. The agreement between the present calculation and that of Williams is better than one part in 10^3 for values of the pressure coefficient, and better than two parts in 10^5 for the lift. We note that the Williams method can only generate test cases, it cannot analyze the flow over a given two-element airfoil.

One use of conformal mapping is to create an efficient coordinate system for transonic-flow calculations, as mentioned in the beginning of the paper. A polar coordinate system in the Z_6 plane of Fig. 7 can be a basis for the calculation of transonic flow over a two-element airfoil. If we create a uniform polar grid, and trace its image back through the transformations to the Z_1 plane, we obtain the results presented in Fig. 9. The airfoils are coordinate lines, and the grid is highly concentrated in the gap between the airfoils. A finer grid would make apparent the grid concentration near the nose of the main airfoil and the trailing edge of the secondary airfoil. The seemingly excessive grid concentration in the gap between the foils can be controlled by the use of a simple stretched grid in the Z_6 plane.

Multiple-Element Airfoil Mapping

The simultaneous conformal transformation of N airfoils in the Z plane into N near circles in the ζ plane may be written as

$$\prod_{j=1}^{N}\left(\frac{\zeta-\zeta_{Tj}}{\zeta-\zeta_{Nj}}\right)=\prod_{j=1}^{N}\left(\frac{Z-Z_{Tj}}{Z-Z_{Nj}}\right)^{1/(2-\tau_j/\pi)} \tag{25}$$

where τ_j = trailing edge included angle of the jth airfoil; Z_{Tj} = trailing edge complex coordinate of the jth airfoil; Z_{Nj} = point midway between nose and center of curvature of the jth airfoil; and where ζ_{Tj} and ζ_{Nj} are appropriately chosen complex constants.

The far-field requirement that

$$\lim_{\zeta\to\infty}(dZ/d\zeta)=1$$

will be satisfied only if

$$\sum_{j=1}^{N}\left[\zeta_{Tj}-\zeta_{Nj}-\left(\frac{Z_{Tj}-Z_{Nj}}{2-\tau_j/\pi}\right)\right]=0 \tag{26}$$

The ζ coordinate system origin can be defined by

$$\zeta_{T1}+\zeta_{N1}=0 \tag{27}$$

Consider the relations

$$f(Z)=\prod_{j=1}^{N}\left(\frac{Z-Z_{Tj}}{Z-Z_{Nj}}\right)^{1/(2-\tau j/\pi)} \tag{28a}$$

and

$$g(\zeta)=\prod_{j=1}^{N}\left(\frac{\zeta-\zeta_{Tj}}{\zeta-\zeta_{Nj}}\right) \tag{28b}$$

The quantity dZ/df will be become infinite when

$$\sum_{j=1}^{N}\left(\frac{1}{2-\tau_j/\pi}\right)\left(\frac{1}{Z-Z_{Tj}}-\frac{1}{Z-Z_{Nj}}\right)=0 \tag{29a}$$

and $d\zeta/dg$ will be infinite when

$$\sum_{j=1}^{N}\left(\frac{1}{\zeta-\zeta_{Tj}}-\frac{1}{\zeta-\zeta_{Nj}}\right)=0 \tag{29b}$$

An analysis shows that in general there are $2N$-2 finite roots of Eq. (29a), all of which are distinct from the Z_{Tj} and Z_{Nj}; similarly, there are $2N$-2 finite roots of Eq. (29b), all of which are distinct from the ζ_{Tj} and ζ_{Nj}. Let these roots be denoted as Z_{0j} and ζ_{0j} for $j=1,\ldots,2N$-2. Then, for $dZ/d\zeta$ and its inverse to be finite at all points distinct from the Z_{Tj}, Z_{Nj}, ζ_{Tj}, and ζ_{Nj}, we must have

$$f(Z_{0j})=g(\zeta_{0j}) \quad j=1,\ldots,2N-2 \tag{30}$$

The $2N$ complex constants ζ_{Tj} and ζ_{Nj} for $j=1,\ldots,N$ are uniquely determined by the $2N$ independent complex constraints given by Eqs. (26-30), and can be calculated using an N-dimensional complex Newton-Raphson iteration. In the case when $N=1$, this reduces to the von Karman-Trefftz transformation.

Conclusions

A number of new conformal mapping concepts have been introduced. The first was the use of a periodic cubic spline to interpolate the airfoil contour in the near-circle plane. The second is the application of fast Fourier techniques to perform rapidly and accurately the Fourier analyses and syntheses required by the Theodorsen-Garrick transformation. The final and perhaps most significant concept is the introduction of a new class of transformations, of which the von Karman-Trefftz transformation is a special case. These new transformations can simultaneously transform multielement airfoils to near circles, or can transform an airfoil to a near circle while transforming a nearby circle to a circle.

References

[1]Sells, C.C.L., "Plane Subcritical Flow Past a Lifting Airfoil," *Proceedings of Royal Society of London,* Vol. 308A, Dec. 1968, pp. 377-401.

[2]Melnik, R.E. and Ives, D.C., "Subcritical Flows over Two-Dimensional Airfoils by a Multistrip Method of Integral Relations," *Proceedings of the Second International Conference on Numerical Methods in Fluid Mechanics, Lecture Notes in Physics,* Vol. 8, Springer-Verlag, New York, 1970, pp. 243-251.

[3]Jameson, A., "Transonic-Flow Calculations for Airfoils and Bodies of Revolution," Grumman Aerospace Corp., Bethpage, N.Y., Aerodynamics Rept. 390-71-7, Dec. 1971.

[4]Bauer, F., Garagedian, P., and Korn, D., "Supercritical Wing Sections," *Lecture Notes in Economics and Mathematical Systems,* Vol. 66, Springer-Verlag, New York, 1972.

[5]Jameson, A., "Iterative Solution of Transonic Flows over Airfoils and Wings, including Flows at Mach 1," *Communications on Pure and Applied Mathematics,* Vol. XXVII, May 1974, pp. 283-309.

[6]Lagally, M., "Die reibungslose Stromung in Aussengebiete zwier Kriese," *Zeitschrift fur Angewandte Mathematik und Mechanik,* Vol. 9, Aug. 1929, pp. 209-305. (translated in NACA TM 626).

[7]Theodorsen, T. and Garrick, I.E., "General Potential Theory of Arbitrary Wing Sections," NACA TR No. 452, 1933.

[8]von Karman, T. and Trefftz, E., "Potential-stromung um gegebene Tragflachenquerschnitte," *Zeitschrift fur Flugtechnische Moforluftsch,* Vol. 9, 1918, pp. 111-116.

[9]Bauer, F., Garabedian, P., Korn, D., and Jameson, A., "Supercritical Wing Sections II," *Lecture Notes in Economics and Mathematical Systems,* Vol. 108, Springer-Verlag, New York, 1975, p. 221.

[10]Ahlberg, J.H., Nilson, E.N., and Walsh, J.L., *The Theory of Splines and Their Applications,* Academic Press, New York, 1967, pp. 9-16.

[11]Cooley, J.W., Lewis, P.A.W., and Welch, P.D., "The Fast Fourier Transform Algorithm: Programming Considerations in the Calculation of Sine, Cosine, and Laplace Transforms," *Journal of Sound and Vibration,* Vol. 12, July 1970, pp. 315-337.

[12]Cooley, J.W. and Tukey, J.W., "An Algorithm for the Machine Calculation of Complex Fourier Series," *Mathematics of Computation,* Vol. 19, April 1965, pp. 297-301.

[13]Garrick, I.E., "Conformal Mapping in Aerodynamics, with Emphasis on the Method of Successive Conjugates," *Symposium on Construction and Applications of Conformal Maps,* National Bureau of Standards, Applied Mathematics Series, Vol. 18, June 1949, pp. 137-147.

[14]Warschawski, S.E., "On Theodorsen's Method of Conformal Mapping of Nearly Circular Regions," *Quarterly of Applied Mathematics,* Vol. 3, April 1945, pp. 12-28.

[15]Abramovici, F., "The Accurate Calculation of Fourier Integrals by the Fast Fourier Transform Technique," *Journal of Computational Physics,* Vol. 11, Jan. 1973, pp. 28-37.

[16]Garrick, I.E., "Potential Flow about Arbitrary Biplane Wing Sections," Rept. 542, NACA, 1936.

[17]Williams, B.R., "An Exact Test Case for the Plane Potential Flow about Two Adjacent Lifting Airfoils," Royal Aircraft Establishment, Farnborough, England, TR 71197, Sept. 1971.